Enhanced tensile strength, fracture toughness and piezoresistive performances of CNT based epoxy nanocomposites using toroidal stirring assisted ultra-sonication

A. Esmaeili[*1, 2,3] C. Sbarufatti[2], K. Youssef[1], A. Jiménez-Suárez[4], A. Ureña[4], A.M.S. Hamouda[3]

[1] Department of Material Science and Technology, College of Art and Science, Qatar University, Doha, Qatar

[2] Politecnico di Milano, Department of Mechanical Engineering, Milan, Italy

[3] Department of mechanical and industrial engineering, College of Engineering, Qatar University, Doha, Qatar

[4]Materials Science and Engineering Area, Escuela Superior de Ciencias Experimentales y Tecnología, Universidad Rey Juan Carlos, Móstoles, Madrid, Spain

Abstract:

The importance of proper CNT dispersion is still the main challenge in CNTs doped epoxy nanocomposites. Therefore, this study was aimed to investigate the effect of toroidal stirring-assisted sonication on final mechanical, electrical and electromechanical properties of the nanocomposites. Two different samples were produced i.e. one with just sonication (M1 batch) and the other was produced using a combination of sonication and high toroidal stirring in an iterative approach (M2 batch). While piezoresistivity performance of the CNT based nanocomposites were mainly investigated in the literature for tensile mode and less attempts were conducted in presence of a pre-crack, both tensile and fracture tests were performed in this study to measure mechanical and electromechanical properties of the nanocomposites. SEM and FESEM were used for the microstructural characterizations. Results showed that M2 batch resulted in a better mechanical, electrical, and piezoresistivity performance than the M1 batch resulting from a better CNT dispersion and less amount of voids in the former compared to the latter. In fact, tensile strength and fracture toughness was increased by 70 % and 17 %, respectively for M2 batch with respect to M1 batch . Moreover, the electrical conductivity and piezoresistive-sensitivity of the M2 batch increased by 5% and 14%, respectively, compared to M1 batch. Finally, different trends in piezoresistivity was revealed in the fracture test before the occurrence of macroscopic damage, attributed to state of CNT dispersion and manifesting as a negative and positive trend for the M2 and M1 batches, respectively.

Keywords: CNT, epoxy, piezoresistivity, tensile strength, fracture toughness

1. Introduction:

[*] **Corresponding Author** :
E-mail addresss: ali.esmaeili@polimi.it, Ali.Esmaeili@qu.edu.qa

Growing demand of high performance materials in many industrial sectors including aerospace and automobile sections has engrossed scientists to engineer multifunctional materials. In this context, epoxy has been extensively used as a promising material for creating novel advanced materials, in particular for Carbon Fiber Reinforced Polymers (CFRPs) and Glass Fiber Reinforced Polymers (GFRPs). This was mainly attributed to its low cost, easy process, and appropriate thermal and mechanical properties [1].

Invention of CNTs by Iijima et al. [2], has shed further light into polymer composites which led to significant amount of research on the effective exploitation of CNTs in enhancing mechanical properties of the epoxy including tensile strength properties [2–9]. However, the susceptibility of epoxy to crack propagation, arisen from its high crosslink density, made it critical for industrial applications, which drives research on the effects of CNTs against crack propagation to prevent catastrophic failure. Since CFRP are being extensively used in safety critical components such as the aircraft fuselage and wing [10], sensing capability of the CNT/epoxy piezoresistive sensor should be evaluated in presence of crack which can be employed for real-time monitoring of damage initiation and extension in an industrial component.

A comprehensive examination was carried by Gojny et al. [2,5] in which they investigated the influence of adding different types of CNTs with different weight concentrations, including SWCNTs, DWCNTs, and MWCNTs, on tensile strength, Young's modulus, and fracture toughness. They have concluded that SWCNT and DWCNT showed higher tendency to agglomerate compared to the MWCNTs, attributed to larger specific surface area in SWCNTs and DWCNTs compared to the MWCNT. However, MWCNTs manifested lower efficiency in improving mechanical properties with respect to SWCNTs and DWCNTs resulting from poor interfacial loading transfer amongst inner tubes. Regardless of the CNT morphology, the enhancement of fracture toughness was more noticeable compared to tensile strength and Young's modulus. However, it was pointed out that increasing CNT contents caused further agglomeration due to higher viscosity of the CNT/epoxy mixture which turned out to reduce the effectiveness of the dispersion method used, thus, optimizing CNT contents is also critical in achieving appropriate mechanical properties. Furthermore, high variations can be identified in mechanical properties, which was attributed to manufacturing defects such as CNT dispersion, poor interfacial bonding between CNTs and matrix, and remaining voids.

Other than to increase the mechanical properties of the material, CNTs also manifested outstanding performance in increasing electrical conductivity of the epoxy in the range of several orders of magnitude with a low percolation threshold, as well as assigning new properties to the matrix, especially piezoresistivity, that can be exploited in the framework of Structural Health Monitoring (SHM) of composite materials [11–18]. Specifically for in-situ SHM, CNTs doped epoxy

nanocomposites manifested sufficient sensitivity to strain in the material, which can be exploited in real-time to monitor the deformation and damage progression in the structure, as an alternative to conventional strain gauges. This is of paramount importance in view of replacement of traditional strain sensors, typically limited to monitor local areas in the vicinity of damage, whilst self-sensing by CNTs doped epoxy is by nature a distributed monitoring approach.

Similarly to their mechanical properties, CNT doped epoxies also experience high variations in their piezoresistive-sensitivities, expressed as the ratio of normalized resistance and strain, typically in the range between 0.3 and 2.9 [14,19–24], depending on the CNT weight concentration and dispersion approaches. Different mechanical dispersion methods were used to produce CNTs doped epoxy, including ultra-sonication, high shear mixing, and calendering methods, each manifesting positive and negative effects on CNT morphology [25]. Sonication also known as ultrasonic homogenizer is the most typical dispersion method used in nanocomposite due to its minimum waste compared to other methods as well as its easy implementation. Nanofillers damage when high sonication time and power are considered is the main drawback of probe-sonication [26]. Three roll mill method, also known as calendering method, is another typical procedure used for nanofiller dispersion in which high shear forces exerted by the rollers caused dispersion of nanofillers. This method was taken into account as the most efficient method in breaking CNT aggregates into smaller pieces especially when viscosity was high [5]. On the other hand, nanofiller wastes and the gap size limitation (1-5μm) made some concerns for effective usage of this method for some applications [25]. Finally, high shear mixing method, also called toroidal method, is another technique used for polymer nanocomposite fabrication. The capability to perform degassing under controlled temperature is the advantage of this method, which is very helpful in efficient removal of air bubbles, in particular, when highly viscous materials are treated. The homogenization effect of this method was also demonstrated by Sánchez-Romate et al. [27] in which an effective breakage of large CNT aggregates into smaller pieces took place. This was related to 3-D shear forces excreted by propeller leading to a better homogenization effect. Besides, chemical functionalization of CNTs is another fator influencing their dispersion states and interfacial bondings with epoxy [25,28,29]. Amino-treatment (CNT-NH_2) and acid treatment of CNTs with carboxylic acid (–COOH) or hydroxyl (–OH) groups known as CNT-COOH or CNT-OH, respectively, are the most common chemical functionalization approach. In this paper, the focus will be on a combined mechanical dispersion approach rather than chemical functionalization of CNTs.

Although some works have discussed the effect of CNT dispersion on mechanical and electromechanical properties of CNT doped epoxy [24,30,31], this still requires further examinations to better interpret the multifunctional properties of CNT doped epoxy under different dispersion techniques and to ensure achieving high performance materials in terms of mechanical and self-

sensing properties. In addition, a majority of the previous works on piezoresistive sensitivity of CNT doped epoxy was conducted in tensile or flexural modes. On the other hand, their piezoresistivity performances in presence of a pre-crack, i.e. in fracture toughness tests, has been rarely addressed, though of large importance as CNT/epoxy nanocomposite are considered as brittle materials.

Therefore, this study aims to investigate the effect of using different dispersion approaches i.e., sonication method with and without toroidal stirring method, on mechanical, electrical, and electromechanical performances of the DWCNT doped epoxy. In a previous study by some of the authors, in which DWCNTs at different loadings (0.5 and 0.75 wt.%) were dispersed by sonication only [14], a better mechanical and piezoresistivity performance was achieved for the former. Thus, a combined iterative approach, i.e., toroidal stirring assisted sonication, is used in this study as an alternative to sonication only. The nanocomposites developed by the two methods were compared based on the states of CNT dispersion, mechanical, electrical, and piezoresistivity performances. SEM and FESEM were used for materials characterization, while tensile and fracture tests were conducted for mechanical and piezoresistivity characterizations.

2. Experimental

2.1. Materials

A combination of SWCNTs-DWCNTs, hereinafter referred to as DWCNTs, purchased from Cheaptubes, is used in this study as conductive nanofiller, specifically with length: 3-30 μm, outer diameter: 1-2 nm, Purity > 99 wt.%, Ash: 0 wt. %. The matrix was composed of a diglycidyl ether of bisphenol A (DGEBA) epoxy with amine hardener, Araldite LY556 resin, and XB3473 hardener purchased from Hunstman, with the mass ratio of 100:23 (LY556:XB3473).

2.2. Nanocomposite preparation

Two different manufacturing approaches were employed for nanocomposite fabrication, as schematically shown in the flowchart in Fig.1. For both methods, a CNT content of 0.5 wt.% was selected to investigate the effect of the change in manufacturing parameters on final mechanical and electromechanical properties. This was selected based on our previous research on the mechanical and piezoresistive characterization of DWCNT/epoxy at different CNT loadings [14].

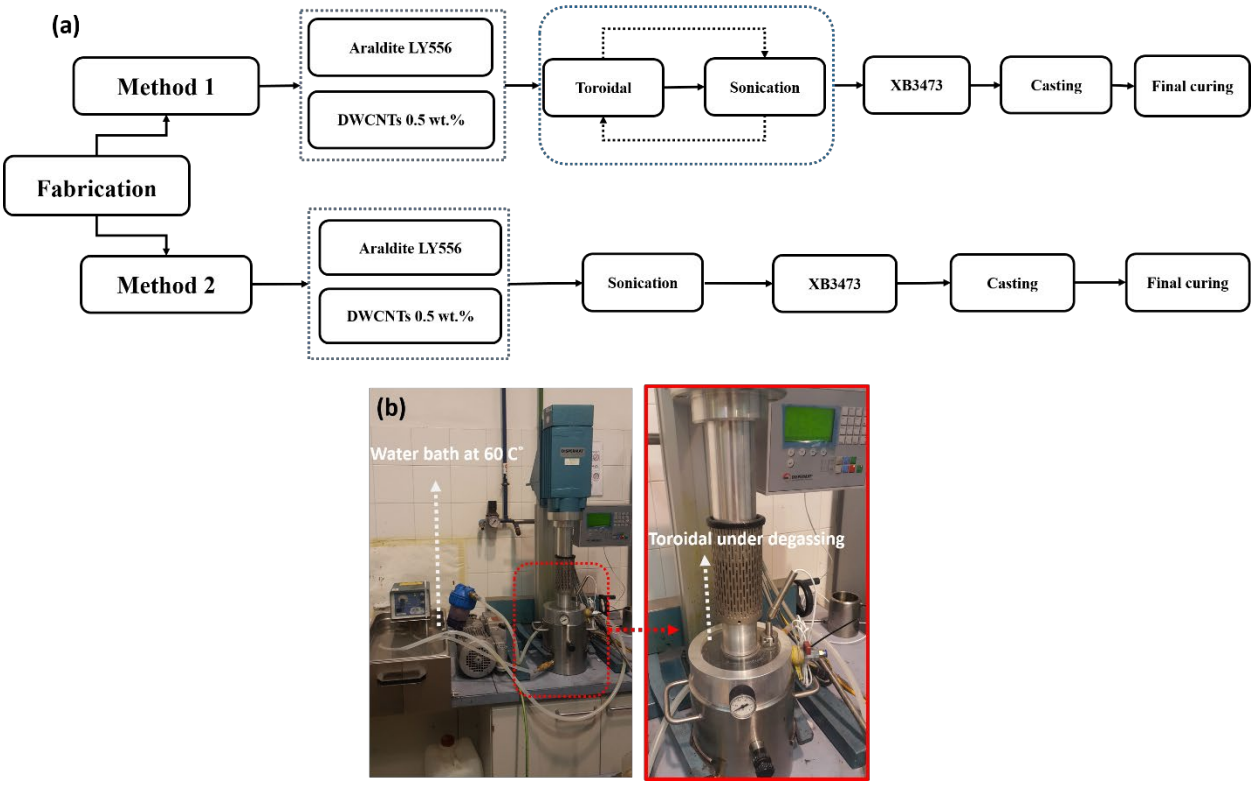

Fig. 1. (a) Manufacturing approaches, (b) toroidal stirring with simultaneous degassing at 60 ˚C

Table 1 shows the dispersion and degassing parameters used in each method. In the first method, named M1, sonication was mainly employed for CNT dispersion, whereas an iterative combined approach using sonication and toroidal methods was used for the second method, hereinafter referred to as M2. The sonication was performed by Hielscher UP400S at 50% amplitude and 0.5 s cycle. In addition, a more effective degassing (Fig.1b) was carried out for the M2 as it was simultaneously performed during the toroidal stirring, thus, making it easier to evacuate air bubbles remained at the bottom side of the mixture. On the other hand, simple vacuum degassing without toroidal stirring was performed for the M1. It is worth noting that the manufacturing parameters used in the M2 were selected based on our previous research on CNT/epoxy and hybrid CNT-nanoclay epoxy nanocomposites [14,23,32,33]. Finally, the hardener was added to the CNT/epoxy mixtures and was cast into an open mold with the dimension of 196 × 145 × 5 mm for final curing at 140 ˚C for 8 h. For the neat epoxy, Part A of the epoxy was first degassed for 30 min at 70 ˚C followed by addition of the hardener for final curing at 140 ˚C for 8 h. It should be noted that the hardener was degassed in the vacuum oven for 30 min prior to addition to the epoxy for both neat and nanocomposite epoxy.

Table 1. Dispersion and degassing approaches

ID	Dispersion	Degassing
Method 1 (M1)	Sonication for 30 min	30 min at 70 ˚C
Method 2 (M2)	(i) toroidal stirring at 5500 rpm for 10 min, (ii) Sonication for 15 min, (iii) toroidal stirring at 2000 rpm for 10 min, (iv) Sonication for 15 min, Toroidal at 50 rpm for 30 min.	Simultaneous degassing during toroidal at 70 ˚C (Fig.1b)

2.3. Characterization

Tensile and Single Edge Notch Bending (SENB) specimens were cut from the casted plates using a waterjet technique according to dimensions shown in ASTM D638 and ASTM D5045 (Fig.2). Six and five specimens were prepared for tensile and fracture tests respectively. It is worth noting that, while during curing the entrapped air moves toward the upper side of the plate to leave the CNT/epoxy mixture, a part of it becomes trapped in the specimen as the material begins to solidify. Thus, the top surfaces of the plates were machined to flatten them and to remove possible porosities that mostly remained at the top surface. Mechanical performance of the nanocomposites was compared based on the tensile strength and the fracture toughness, i.e., critical stress intensity factor (K_{IC}). K_{IC} was calculated according to Equation 1. A pre-crack was created into the SENB specimen by sliding a fresh razor blade to guarantee the real fracture toughness properties are obtained, always assuring the ratio (x) of total crack length (a) and specimen width (w), Equation 2, was bounded as $0.45 < x < 0.55$.

$$K_Q = \left(\frac{P_Q}{BW^{\frac{1}{2}}}\right) f(x) \qquad (1)$$

$$x = \frac{a}{w} \qquad (2)$$

$$B, a, (W - a) > 2.5\left(\frac{K_Q}{\sigma_y}\right)^2 \qquad (3)$$

B is the thickness [mm], W the width [mm], a total crack length [mm], K_Q conditional K_{IC} [MPa.m$^{0.5}$], $f(x)$ a calibration factor is given in ASTM D5045.

It is worth noting that equation (3), called size criteria, was met for all samples, meaninig a valid K_{IC} was obtained for all the specimens. Tensile and fracture tests were carried out using MTS Alliance RF150 and MTS Synergie 200A electromechanical testing machines, respectively, with a crosshead speed of 0.5 mm/min. SEM (Zeiss EVO 50) and FESEM (Zeiss SUPRA 40) were employed for dispersion analysis and fractography, after gold deposition on the analised surfaces for better conductivity and imaging.

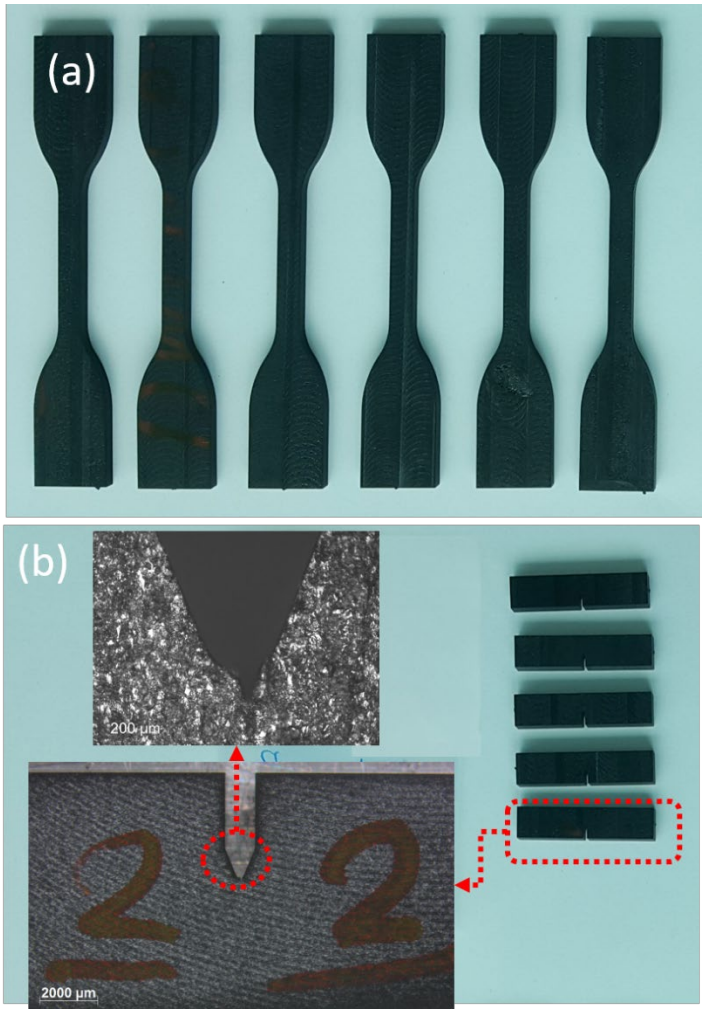

Fig. 2. Sample configuration: (a) Dog-bone specimen, (b) SENB specimen

the samples. Voltage of 1 to 100 V was applied, and the current density was read. Samples were subjected to a steady pressure by means of a fixture to guarantee appropriate and consistent contact between the electrodes and samples was provided. For piezoresistivity characterization, a two-probe technique was employed to investigate the strain sensing performance of the nanocomposites using two electrodes placed at distance of 50 and 30 mm for the tensile and SENB specimen, respectively. A silver paste was applied to the electrode/specimen joint to reduce the contact resistance. A steady current of 0.200 μA was applied between contacts using a power supply STAB AR60. The change in output signal (voltage) was recorded in real-time using Data Acquisition System NI9234 (DAQ) plugged into a laptop running Ni Signal Express software. Finally, the normalized resistance change and sensitivity of the developed strain sensor were obtained according to equations 5 and 6.

$$\Delta R_n = \frac{\Delta R}{R_0} = \frac{R_t - R_0}{R_0} = \frac{V_t - V_0}{V_0} \quad (5) \quad [23]$$

$$G.F. = \frac{\Delta R_n}{\varepsilon} \quad (5) \quad [23]$$

Where V_0 and R_0 are the initial voltage [mV] and resistance [Ω], V_t [mV] and R_t [Ω] the instantaneous voltage and electrical resistance, which are expected to change by the strain increase and damage evolution in the system; ΔR_n normalized resistance [Ω], ε the applied strain during the tensile test [-] measured by an extensometer, and $G.F.$ the gauge factor or sensitivity [-].

3. Results and discussion

3.1. CNT dispersion

Fig. 3a-b and c-d show the state of CNT dispersion on the fracture surface of the tensile and SENB specimens respectively. The presence of CNT aggregate as marked by red arrows is clear for the nanocomposite produced by M1. In contrast, a good CNT dispersion is achieved for the samples produced by M2 i.e., the latter can successfully reach a better CNT dispersion with respect to the former. This can be attributed to the high swirling velocity flow applied to the CNT aggregates by a rotating blade, which breaks the larger CNT aggregates into smaller pieces, thus, avoiding CNT reagglomeration while mixing the nanomaterials [22].

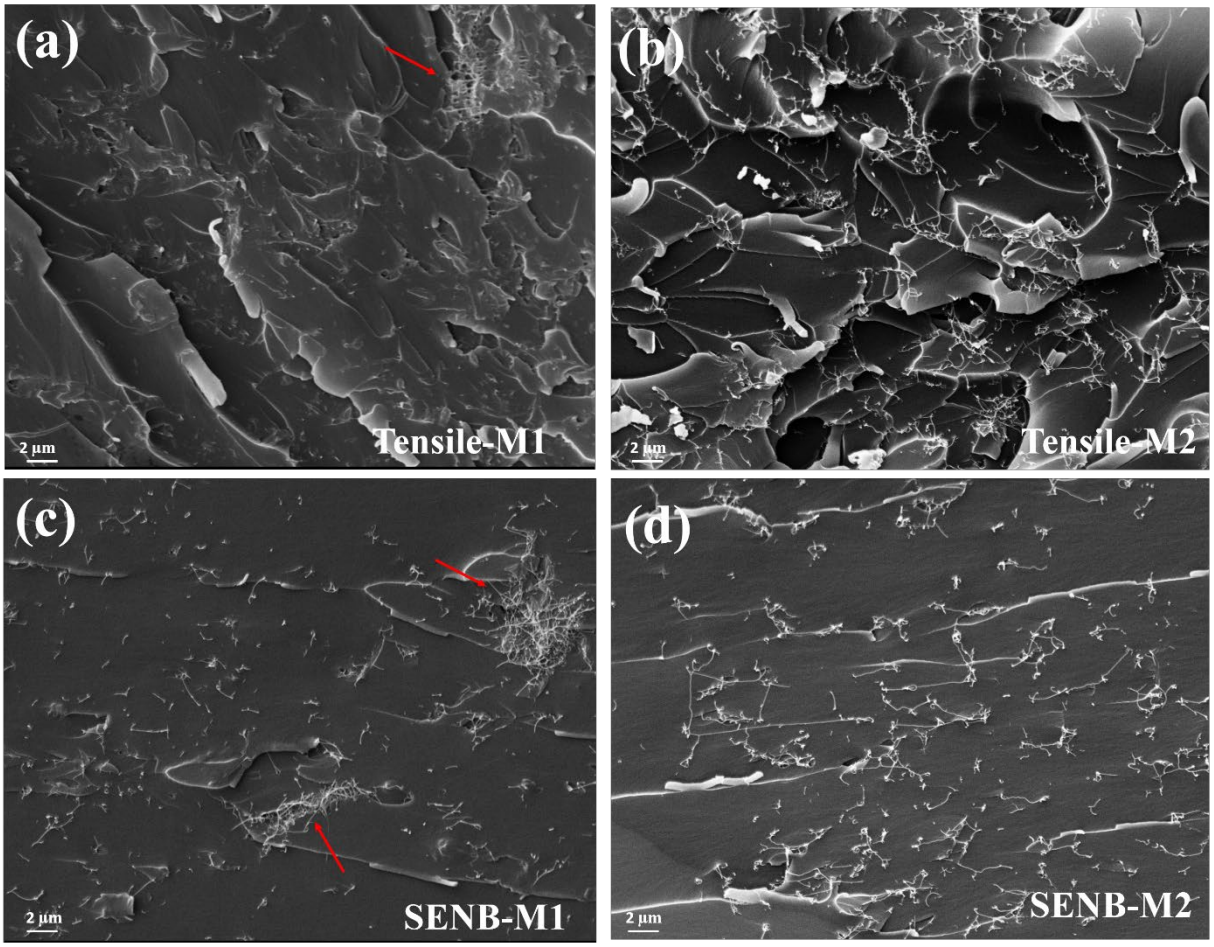

Fig. 3. SEM image of the CNT dipesrion : (a-b) tensile, (c-d) SENB specimens (left and right figures represent samples produced by M1 and M2 respectively)

3.2. Voids

Fig.4 show FESEM images of the fracture surface of the tensile specimens. The presence of manufacturing defects such as voids is quite tangible for the samples produced by the M1 as many tiny holes can be clearly seen within the fracture surface as shown by the red arrows in Fig.4a and c. On the other hand, no voids or bubbles are noticed for the sample produced by M2 (Fig.4b and d). This can be attributed to a better degassing procedure performed in M1 compared to M2 i.e., simultaneous degassing under toroidal stirring can mitigate better evacuation of the air bubbles, especially those that remain at the bottom area [33–35]. It should be noted that although the same temperature was used for both methods, the viscosity of the mixture hampers efficient evacuation of the air, especially those remained at the bottom side; thus, the high swirly flow imposed by the toroidal disk can shift them up resulting in a more efficient degassing. It can be concluded that

toroidal stirring not only improves CNT dispersion but it also leads to a better evacuation of the air from the mixture.

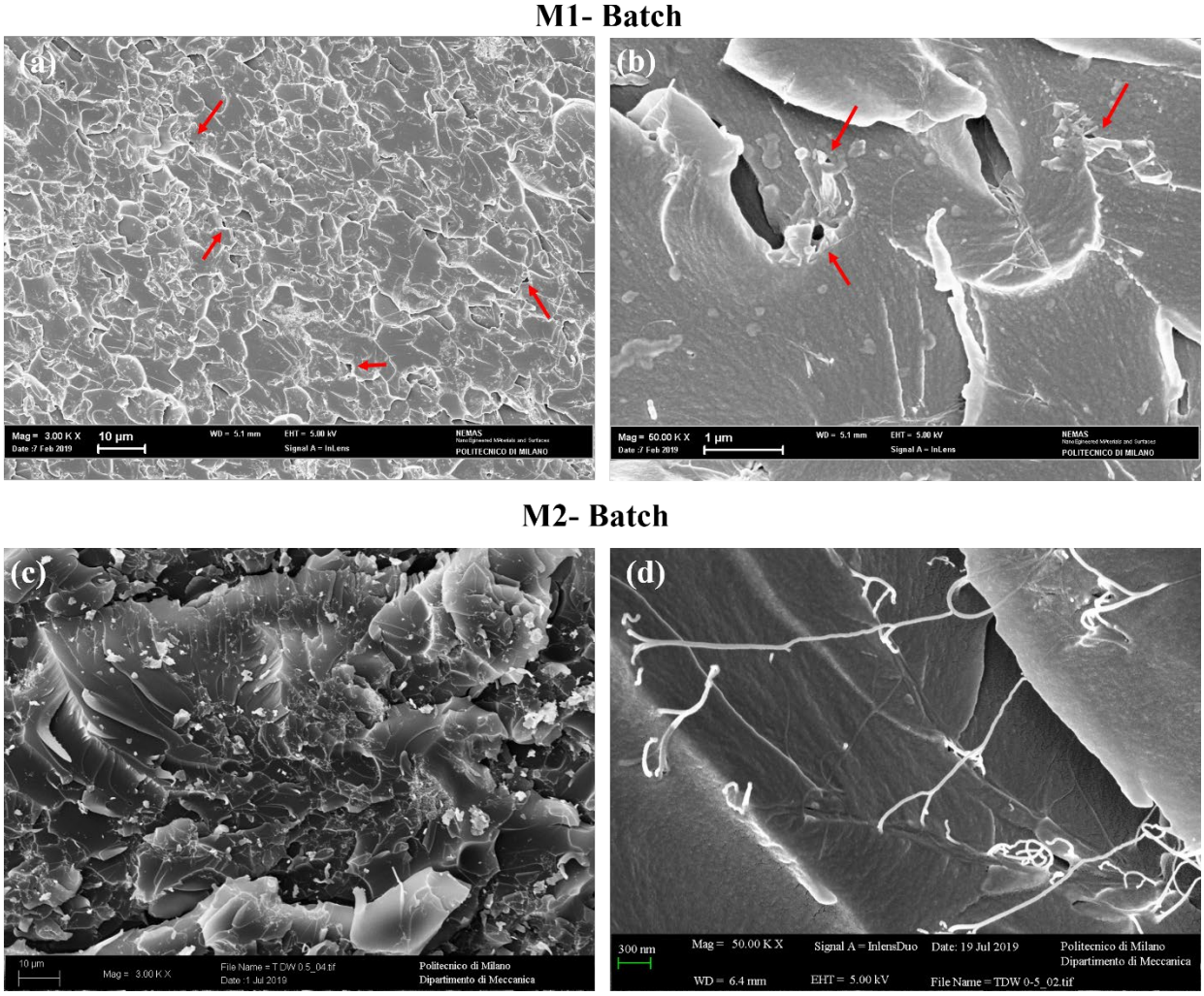

Fig. 4. FESEM image of the fracture surface of tensile specimen: (a-b) M1, (c-d) M2, red arrows point to presence of voids.

3.3. Mechanical properties

Table 2 shows the mechanical properties of the developed nanocomposites and the neat epoxy, along with their standard deviation interval. The nanocomposite produced by M2 manifested higher mechanical properties compared to the ones developed by M1. In fact, an increase of 70 % and 17 % in tensile strength and fracture toughness, respectively, are achieved for the nanocomposites manufactured by M2 with respect to the M1.

Table 2. Mechanical properties

Materials	Tensile strength (MPa)	Fracture toughness (MPa.m$^{0.5}$)
Neat epoxy	52 ±3	0.77±0.1
M1	30 ±8	1.11±0.07
M2	53±3	1.3±0.04

Likewise, a lower tensile strength, 44 % reduction, is obtained for M1 with respect to the neat epoxy, though the tensile strength of the M2 did not show any reduction compared to the neat epoxy. Severe reduction of the tensile strength of the M1 can be attributed to the formation of voids and higher number of aggregates within the matrix (Fig. 3 and 4) due to inappropriate manufactruing method. Unlike the tensile strength of M1, which is drastically lower than the neat epoxy, the fracture toughness is enhanced by 44 % compared to the neat epoxy. This can be related to the test configuration, i.e. the SENB specimen is subject to a localized stress whilst a global stress distribution is applied to the dog-bone specimen during the tensile test [23]. As a consequence, the SENB specimen will not be significantly impacted by the presence of voids. In addition, from Fig. 4, a cleavage pattern, which is a typical fracture patterns for brittle materials, can be distinguished for all samples, though a higher surface roughness manifested for the specimen produced by M2 compared to M1. It is worthwhile noting that the higher surface roughness correlates to a higher tensile strength and vice versa [33] i.e. higher plastic deformation was taking place before final failure.

Significant improvement of fracture toughness of the nanocomposites with respect to the neat epoxy can be related to the crack-bridging mechanism, which is a typical toughening mechanism for CNT doped epoxy nanocomposites (Fig. 5). In this context, higher energy is required for crack-opening and propagation due to the fact that bridging-CNTs limits damage progression; thus, fracture toughness increases [36]. In addition, as shown in Fig. 5, an appropriate interfacial CNT/epoxy bonding occurred, indicating a successful shear-loading transfer between the CNTs and the epoxy. This can also be proven by the stretching condition of the CNT during loading, manifesting as a change of diameter at the interface and at mid-length, as indicated by white arrows in Fig. 5. Finally, as mentioned before, the nanocomposite fabricated by M2 manifested higher tensile strength and surface roughness compared to M1. The higher fracture surface roughness can be explained by higher deviation of crack-front during propagation (Fig. 3c-d) due to the fact that CNTs act as a barrier against crack propagation. In other words, the crack-front has to either bend around the CNTs or cross through them, which makes the surface more rough. This process also leads to higher dissipation of energy and, as a consequence, fracture toughness is increased.

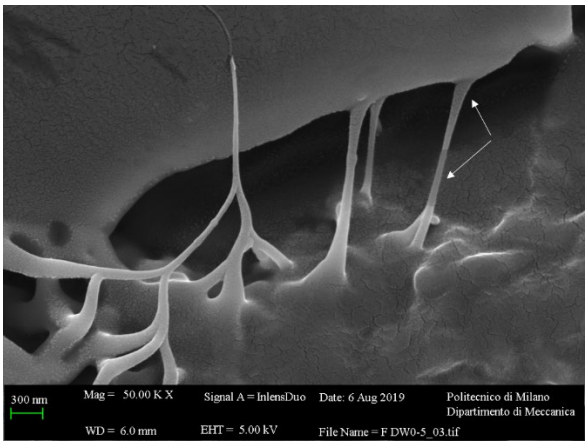

Fig. 5. Crack-bridging mechanism of CNTs

3.4. Electrical conductivity

Fig. 6 shows the electrical conductivity of the samples. Regardless of the manufacturing procedures used, electrical conductivities increase by nine orders of magnitude with respect to the neat epoxy with the conductivity of 10^{-11} S/m. In addition, M2 manifests a limited increase (5.5 %) in electrical conductivity compared to the M1 batch, which again can be attributed to its better CNT dispersion, as shown in Fig. 3. It is worth noticing that tunneling effect among neighboring CNTs, direct electrical contact between CNTs and intrinsic electrical conductivity of CNT are accounted for the significant increase in electrical conductivity, though tunneling effect plays the dominant role [23]. This was well addressed in the literature indicating the electrical conductivity of the CNTs doped epoxy exponentially increases at percolation threshold region, 0.1 to 0.3 wt.% CNTs, in which tunneling effect amongst neighbouring CNTs plays the predominant mechanism [37]. Although in a previous study by the authors a percolation threshold in the range 0.2-0.3 wt.% CNTs was identified for the DWCNT/epoxy [14], an increased amount of CNTs (0.5 wt.%) was used in this research to achieve improved mechanical properties. It can be concluded that although the CNT dispersion was improved in M2 batch compared to M1 batch, this cannot play a significant role in improving conductivity as the CNT content used are far above the percolation threshold. This is in line with our previous results indicating that increasing DWCNT content above percolation threshold led to negligible increase of electrical conductivity, though with a more consistent formation of agglomerates [14].

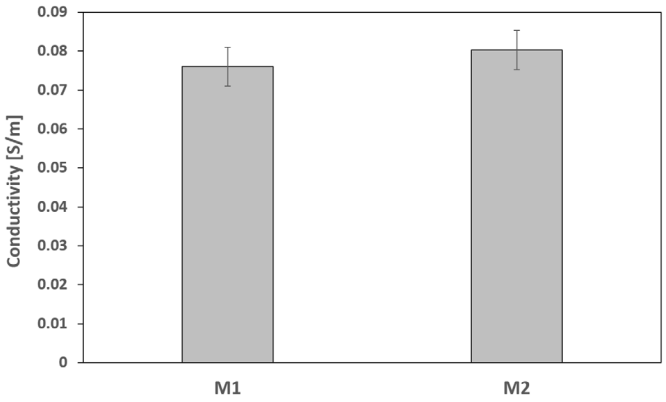

Fig. 6. Electrical conductivity for the samples produced by M1 and M2

3.5. Piezoresistivity

CNTs induce self-sensing properties to the host material, which can be used for strain sensing applications. Specifically, Fig. 7a shows the piezoresistivity performance of the nanocomposite during the tensile test. First, the normalized resistance increases in response of a strain increase which can be attributed to breakage of the electrical pathways resulting from tunneling distance increase and loss of electrical contacts [38,39]. Second, two different trends can be seen for both nanocomposites, including a nonlinear trend at low strain followed by a linear trend at high strain. This indicates that, at low strain, tunneling resistance mainly drives the piezoresistivity whilst a combination of tunneling resistance and loss of electrical contacts amongst neighboring CNTs drives the piezoresistivity at higher strain levels, reducing the slope of the curves [14]. Finally, M2-nanocomposites manifest a better strain sensing compared to M1, arisen from their better CNT dispersion. In fact, the highest sensitivity of 2.6 [-] for a strain of 0.01 [-] is obtained for the nanocomposites produced by M2 (Fig. 7b) whereas a sensitiy of . It should be noted that sensitivity value begins to increase by increasing strain up to a strain value of 0.01 [-], when a nonlinear piezoresistivity can be seen, which is approximately the elastic/plastic transition limit for the nanocomposite material, followed by a constant value (linear trend). Therefore, the sensitivity of the samples at a strain of 0.01 [-] are higher than that for a strain around 0.005 [-], as illustrated in Fig.7 b.

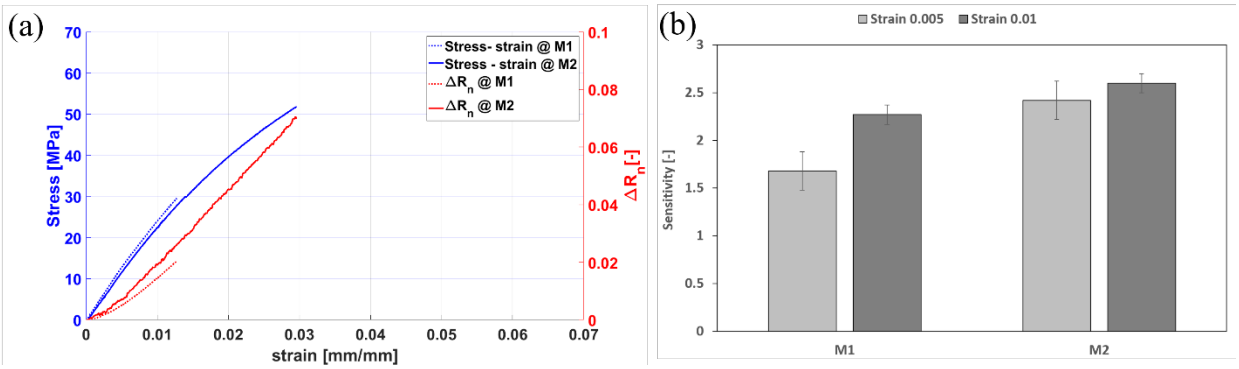

Fig. 7. (a) Piezoresistivity behaviour of the nanocomposites during tensile test, (b) sensitivity

The piezoresistivity performance of the nanocomposite during the fracture test is shown in Fig. 8. Since the change in normalized resistance before and after crack propagation is very large, they are shown separately in Fig. 8(a) and Fig. 8(b), respectively. Before entering into the discussion of the experimental results, it should be noted that a combination of positive and negative variations in normalized resistance is expected for the tension and compression sides, respectively, during the three-point bending test. This is visible in Fig. 9(c), where a finite element simulation of the SENB specimen is used to predict the sign of the strain field axial component. New electrical pathways form in the compression side due to reorientation of CNTs whilst breakages of the electrical networks are more common in tension side [22,32]. As a result, the normalized resistance in fracture test before failure (Fig.8a) is dramatically decreased compared to its value in tensile test i.e. the normalized resistance reduces by 2 order of magnitudes with respect to the tensile test condition, indicating a significant effect of formation of new electrical paths in the SENB bending test.

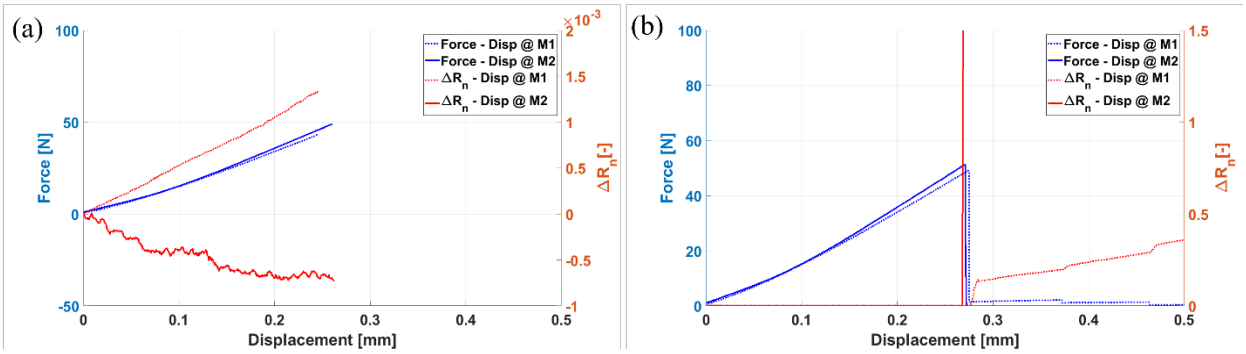

Fig. 8. Piezoresistivity behaviour during fracture test: (a) before crack extension, (b) after failure

From Fig. 8a, it can be seen that for the samples produced by M2, the normalized resistance decreases as a function of displacement while an increasing trend is noticed for M1. This contradictory behaviour can be attributed to improper CNT dispersion in M1 batch compared to M2 as shown in Fig.9 where the red and blue lines represent the electrical pathways in the compression and tension

sides, respectively. Fig.9a suggests the possibility for creation of new electrical pathways in the compression side for M1 batch is less, due to presence of the aggregates, resulting in the augmented distance among CNTs preventing the creation of new electrical pathways: a positive trend in piezoresistivity is eventully obtained, mainly related to CNTs augmenting their relative distance in the tension side. In addition, formation of micro-cracks in the vicinity of CNT aggregates and poor bonding between the epoxy and CNTs can further increase piezoresistivity, even in the compression side [14,23].

On the other hand, a more homogenous CNT dispersion for the M2 batch, resulted in higher possibility for creation of new electrical networks in the compression side, intuitively represented as an higher numbers of red lines in Fig.9b. This leads to a more balanced piezoresistivity with a slight negative trend for M2 compared to the marked positive trend obtained for M1 batch. Furthermore, as shown by the green arrow in Fig.9b, formation of new electrical paths in the tension side is also possible at lower strain levels due to reorientation of CNTs [40]. It can be concluded that, for a very homogenous sample as the M2 batch in this study, contribution of the compression side in piezoresistivity is more dominant than the tension side for a very low strain. Similar results were obtaind in a study made by Sánchez-Romate et al. [22] where a negative piezoresistivity was obtained for a CNT/epoxy thin film coated on the surface of GFRP plate.

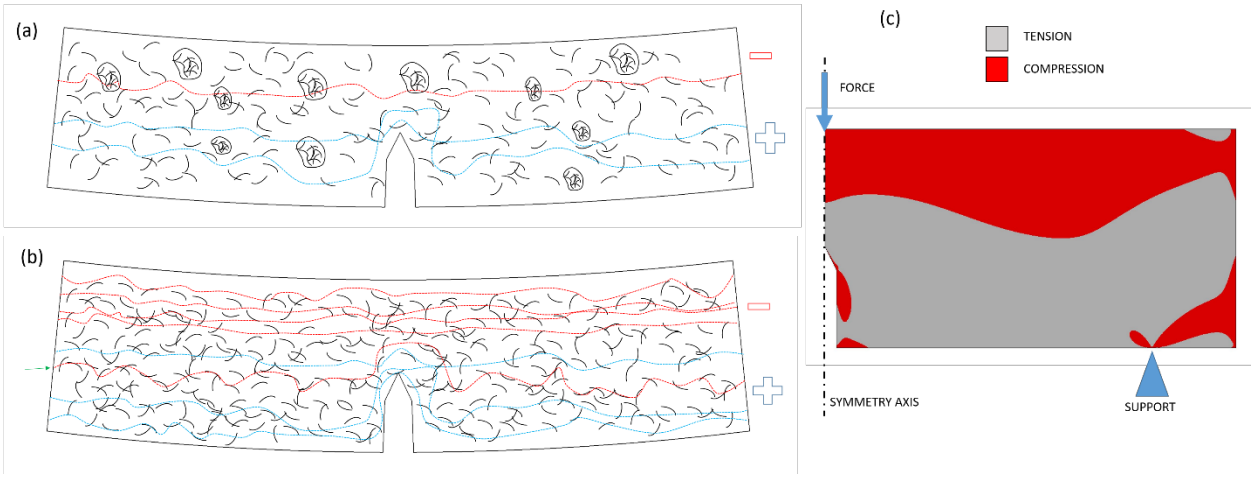

Fig. 9. (a-b) Schematic illustration of formation and breakage of electrical pathways during fracture test in M1 and M2 batches respectively, (c) tension and compression stress distributions in the SENB specimen, results based on finite element analysis.

On the other hand, an abrupt increase in normalized resistance can be seen once the crack extension takes place (for both samples), indicating the main specimen failure (Fig. 8b). It should be noted that the nanocomposite produced by M1 did not fail completely upon first crack extension and some

further step by step pattern is noticed. Accordingly, the normalized resistance versus displacement show the same trend.

In total, based on the achieved electrical, mechanical, and electromechanical properties of the developed nanocomposites, it can be concluded that the optimized manufacturing methodology used in M2 can successfully tailor aforementioned properties. In other words, achieving better CNT dispersion as well as less numbers of voids are the key factors in enhancing multifunctional properties, which is demonstrated throughout this study.

Conclusion

In this study, two nanocomposites were produced using different dispersion and degassing techniques. Results showed that the toroidal stirring method with simultaneous degassing (M2) reached a more omogeneous CNT dispersion compared to the case when only sonication was used (M1). This was related to the breakage of CNT aggregates into smaller pieces by using toroidal stirring. Samples produced by M1 contained a higher amount of pores with respect to samples produced by M2, which resulted in a severe reduction of the tensile strength for the former, even lower than the neat epoxy. As a consequence of the improved CNT dispersion of M2, tensile strength and fracture toughness increased by 70 % and 17 %, respectively, with respect to samples produced by M1. The electrical conductivity of the M2 batch showed a slight increase compared to M1 batch. Crack-bridging was deemed to be responsible for the significant increase of fracture toughness in M2. Piezoresistivity of the M2 nanocomposites showed a better performance during tensile test, where a sensitivity of 2.6 was achieved. Finally, the M2 batch nanocomposite showed a different trend in piezoresistivity (negative) with respect to the M1 batch (positive) before crack extension, which was attributed to the dominating effect of creation of new electrical pathways in the compression side, with respect to their breakage in the tension side.

Acknowledgment

This publication was made possible by GSRA grant No. GSRA2-1-0609-14024 from the Qatar National Research fund (a member of Qatar foundation). The findings achieved herein are solely the responsibilities of the authors.

References:

[1] Liu S, Chevali VS, Xu Z, Hui D, Wang H. A review of extending performance of epoxy resins using carbon nanomaterials. Compos Part B Eng 2018;136:197–214. doi:10.1016/j.compositesb.2017.08.020.

[2] Gojny FH, Wichmann MHG, Fiedler B, Schulte K. Influence of different carbon nanotubes on the mechanical properties of epoxy matrix composites - A comparative study. Compos Sci Technol 2005;65:2300–13. doi:10.1016/j.compscitech.2005.04.021.

[3] Hernández-Pérez A, Avilés F, May-Pat A, Valadez-González A, Herrera-Franco PJ, Bartolo-Pérez P. Effective properties of multiwalled carbon nanotube/epoxy composites using two different tubes. Compos Sci Technol 2008;68:1422–31. doi:10.1016/j.compscitech.2007.11.001.

[4] Quaresimin M, Schulte K, Zappalorto M, Chandrasekaran S. Toughening mechanisms in polymer nanocomposites: From experiments to modelling. Compos Sci Technol 2016;123:187–204. doi:10.1016/j.compscitech.2015.11.027.

[5] Gojny FH, Wichmann MHG, Köpke U, Fiedler B, Schulte K. Carbon nanotube-reinforced epoxy-composites: Enhanced stiffness and fracture toughness at low nanotube content. Compos Sci Technol 2004;64:2363–71. doi:10.1016/j.compscitech.2004.04.002.

[6] Moradi E, Zeinedini A. On the mixed mode I/II/III inter-laminar fracture toughness of cotton/epoxy laminated composites. Theor Appl Fract Mech 2020;105:102400. doi:10.1016/j.tafmec.2019.102400.

[7] Zeinedini A, Shokrieh MM, Ebrahimi A. The effect of agglomeration on the fracture toughness of CNTs-reinforced nanocomposites. Theor Appl Fract Mech 2018;94:84–94. doi:10.1016/j.tafmec.2018.01.009.

[8] Zeinedini A. A novel fixture for mixed mode I/II/III fracture testing of brittle materials. Fatigue Fract Eng Mater Struct 2019;42:838–53. doi:doi:10.1111/ffe.12955.

[9] Subhani T, Latif M, Ahmad I, Rakha SA, Ali N, Khurram AA. Mechanical performance of epoxy matrix hybrid nanocomposites containing carbon nanotubes and nanodiamonds. Mater Des 2015;87:436–44. doi:10.1016/j.matdes.2015.08.059.

[10] De Vivo B, Lamberti P, Tucci V, Guadagno L, Vertuccio L, Vittoria V, et al. Comparison of the Physical Properties of Epoxy-Based Composites Filled with Different Types of Carbon Nanotubes for Aeronautic Applications. Adv Polym Technol 2012;32:474–85. doi:10.1002/adv.

[11] Diamanti K, Soutis C. Structural health monitoring techniques for aircraft composite structures. Prog Aerosp Sci 2010;46:342–52. doi:10.1016/j.paerosci.2010.05.001.

[12] Tuloup C, Harizi W, Aboura Z, Meyer Y, Khellil K, Lachat R. On the use of in-situ piezoelectric sensors for the manufacturing and structural health monitoring of polymer-matrix composites: A literature review. Compos Struct 2019;215:127–49. doi:10.1016/J.COMPSTRUCT.2019.02.046.

[13] Forintos N, Czigany T. Multifunctional application of carbon fiber reinforced polymer composites: Electrical properties of the reinforcing carbon fibers – A short review. Compos Part B Eng 2019;162:331–43. doi:10.1016/j.compositesb.2018.10.098.

[14] Esmaeili A, Urena A, Hamouda AM. Piezoresistive characterization of epoxy based nanocomposites loaded with SWCNTs-DWCNTs in tensile and fracture tests 2020:1–12. doi:10.1002/pc.25558.

[15] Wang Q, Dai J, Li W, Wei Z, Jiang J. The effects of CNT alignment on electrical conductivity and mechanical properties of SWNT/epoxy nanocomposites. Compos Sci Technol 2008;68:1644–

8. doi:10.1016/j.compscitech.2008.02.024.

[16] Allaoui A, Bai S, Cheng HM, Bai JB. Mechanical and electrical properties of a MWNT / epoxy composite. Compos Sci Technol 2002;62:1993–8.

[17] Jang AY, Lim SH, Kim DH, Yun H Do, Lee GC, Seo SY. Strain-Detecting properties of hybrid PE and steel fibers reinforced cement composite (Hy-FRCC) with Multi-Walled carbon nanotube (MWCNT) under repeated compression. Results Phys 2020;18:103199. doi:10.1016/j.rinp.2020.103199.

[18] Li Y, Sun B, Sockalingam S, Pan Z, Lu W, Chou TW. Influence of transverse compression on axial electromechanical properties of carbon nanotube fibers. Mater Des 2020;188:108463. doi:10.1016/j.matdes.2019.108463.

[19] Cao X, Wei X, Li G, Hu C, Dai K, Guo J, et al. Strain sensing behaviors of epoxy nanocomposites with carbon nanotubes under cyclic deformation. Polym (United Kingdom) 2017;112:1–9. doi:10.1016/j.polymer.2017.01.068.

[20] Vertuccio L, Guadagno L, Spinelli G, Lamberti P, Tucci V, Russo S. Piezoresistive properties of resin reinforced with carbon nanotubes for health-monitoring of aircraft primary structures. Compos Part B Eng 2016;107:192–202. doi:10.1016/j.compositesb.2016.09.061.

[21] Spinelli G, Lamberti P, Tucci V, Vertuccio L, Guadagno L. Experimental and theoretical study on piezoresistive properties of a structural resin reinforced with carbon nanotubes for strain sensing and damage monitoring. Compos Part B Eng 2018;145:90–9. doi:10.1016/j.compositesb.2018.03.025.

[22] Sánchez-Romate XF, Moriche R, Jiménez-Suárez A, Sánchez M, Prolongo SG, Güemes A, et al. Highly sensitive strain gauges with carbon nanotubes: From bulk nanocomposites to multifunctional coatings for damage sensing. Appl Surf Sci 2017;424:213–21. doi:10.1016/j.apsusc.2017.03.234.

[23] Esmaeili A, Sbarufatti C, Ma D, Manes A, Jiménez-Suárez A, Ureña A, et al. Strain and crack growth sensing capability of SWCNT reinforced epoxy in tensile and mode I fracture tests. Compos Sci Technol 2020;186. doi:10.1016/j.compscitech.2019.107918.

[24] Tanabi H, Erdal M. Effect of CNTs dispersion on electrical, mechanical and strain sensing properties of CNT/epoxy nanocomposites. Results Phys 2019;12:486–503. doi:10.1016/j.rinp.2018.11.081.

[25] Ma PC, Siddiqui NA, Marom G, Kim JK. Dispersion and functionalization of carbon nanotubes for polymer-based nanocomposites: A review. Compos Part A Appl Sci Manuf 2010;41:1345–67. doi:10.1016/j.compositesa.2010.07.003.

[26] Lu KL, Lago RM, Chen YK, Green MLH, Harris PJF, Tsang SC. Mechanical damage of carbon nanotubes by ultrasound. Carbon N Y 1996;34:814–6.

[27] Sánchez-romate XF, Artigas J, Jiménez-suárez A, Sánchez M, Güemes A, Ureña A. Critical parameters of carbon nanotube reinforced composites for structural health monitoring applications : Empirical results versus theoretical predictions. Compos Sci Technol 2019;171:44–53. doi:10.1016/j.compscitech.2018.12.010.

[28] Liu X, Liu W, Xia Q, Feng J, Qiu Y, Xu F. Highly tough and strain sensitive plasma functionalized carbon nanotube/epoxy composites. Compos Part A Appl Sci Manuf 2019;121:123–9. doi:10.1016/j.compositesa.2019.03.015.

[29] Cha J, Jun GH, Park JK, Kim JC, Ryu HJ, Hong SH. Improvement of modulus, strength and fracture toughness of CNT/Epoxy nanocomposites through the functionalization of carbon nanotubes. Compos Part B Eng 2017;129:169–79. doi:10.1016/j.compositesb.2017.07.070.

[30] Li J, Ma PC, Chow WS, To CK, Tang BZ, Kim JK. Correlations between percolation threshold, dispersion state, and aspect ratio of carbon nanotubes. Adv Funct Mater 2007;17:3207–15. doi:10.1002/adfm.200700065.

[31] Montazeri A, Chitsazzadeh M. Effect of sonication parameters on the mechanical properties of multi-walled carbon nanotube/epoxy composites. Mater Des 2014;56:500–8. doi:10.1016/j.matdes.2013.11.013.

[32] Synergistic effects of double-walled carbon nanotubes and nanoclays on mechanical , electrical and piezoresistive properties of epoxy based nanocomposites 2020;200:1–11. doi:10.1016/j.compscitech.2020.108459.

[33] Esmaeili A, Ma D, Manes A, Oggioni T, Jiménez-suárez A, Ureña A, et al. An experimental and numerical investigation of highly strong and tough epoxy based nanocomposite by addition of MWCNTs : Tensile and mode I fracture tests 2020;252. doi:10.1016/j.compstruct.2020.112692.

[34] Hamouda AMS, Rovatti L, Ure A. Synergistic effects of double-walled carbon nanotubes and nanoclays on mechanical , electrical and piezoresistive properties of epoxy based nanocomposites 2020;200:1–11. doi:10.1016/j.compscitech.2020.108459.

[35] Ure A, Hamouda AMS. Effective addition of nanoclay in enhancement of mechanical and electromechanical properties of SWCNT reinforced epoxy : Strain sensing and crack-induced piezoresistivity 2020;110. doi:10.1016/j.tafmec.2020.102831.

[36] Ayatollahi MR, Shadlou S, Shokrieh MM. Fracture toughness of epoxy/multi-walled carbon nanotube nano-composites under bending and shear loading conditions. Mater Des 2011;32:2115–24. doi:10.1016/j.matdes.2010.11.034.

[37] Hu N, Karube Y, Yan C, Masuda Z, Fukunaga H. Tunneling effect in a polymer / carbon nanotube nanocomposite strain sensor 2008;56:2929–36. doi:10.1016/j.actamat.2008.02.030.

[38] Simmons JG. Generalized Formula for the Electric Tunnel Effect between Similar Electrodes Separated by a Thin Insulating Film. J Appl Phys 1963;34:1793–803. doi:10.1063/1.1702682.

[39] Oskouyi AB, Sundararaj U, Mertiny P. Tunneling conductivity and piezoresistivity of composites containing randomly dispersed conductive nano-platelets. Materials (Basel) 2014;7:2501–21. doi:10.3390/ma7042501.

[40] Mahmood H, Vanzetti L, Bersani M, Pegoretti A. Mechanical properties and strain monitoring of glass-epoxy composites with graphene-coated fibers. Compos Part A Appl Sci Manuf 2018;107:112–23. doi:10.1016/j.compositesa.2017.12.023.